Multi-proxy palaeoenvironmental reconstruction of the Skagerrak from the Lateglacial to Middle Holocene

EMMA OWNSWORTH (iD), MATTHIAS MOROS (iD), JEREMY LLOYD, OLE BENNIKE (iD), JØRN BO JENSEN, THOMAS BLANZ AND DAVID SELBY

This study uses a multiproxy approach including the first use of $^{187}Os/^{188}Os$, $\%C_{37:4}$ biomarkers, carbonate content, sedimentological grain size, geochemical X-ray fluorescence and microfossil benthic foraminifera species combined with radiocarbon dating, measured on six cores from across the Skagerrak, in order to study the Lateglacial to Middle Holocene history of the area. A new chronostratigraphic framework is developed based on the appearance of specific benthic foraminifera species along with changes in carbonate/X-ray fluorescence and grain size data. This allowed the correlation of cores based on a series of radiocarbon dated tie points. Analysing the cores together reveals several events recorded in the Skagerrak including: (i) an increased freshwater input (bracketed between 13.3 and 11.3 cal. ka BP) signified by radiogenic $^{187}Os/^{188}Os$ values, high $\%C_{37:4}$ values and an increase in sand content; (ii) the Glomma drainage event, signified by a sudden appearance of *Valvulineria* as well as higher $\%C_{37:4}$; and (iii) the opening of the Danish Straits and English Channel leading to the development of modern-day conditions and circulation patterns in the Skagerrak, signified by the appearance of *Hyalinea balthica* and a fall in $\%C_{37:4}$.

Emma Ownsworth (e.m.ownsworth@durham.ac.uk) and David Selby, Department of Earth Sciences, Durham University, Durham DH1 3LE, UK; Matthias Moros, Leibniz Institute for Baltic Sea Research Warnemünde, Seestrasse 15, D-18119 Rostock, Germany; Jeremy Lloyd, Department of Geography, Durham University, Durham DH1 3LE, UK; Ole Bennike and Jørn Bo Jensen, Geological Survey of Denmark and Greenland (GEUS), Universitesbyen 81, DK-8000 Aarhus C, Denmark; Thomas Blanz, Institute of Geosciences, Department of Geology, Kiel University, Ludewig-Meyn Strasse 10, D-24118 Kiel, Germany; received 28th April 2023, accepted 21st January 2024.

Throughout the late Quaternary and Holocene the palaeogeography of the Baltic Sea Basin, Skagerrak and surrounding areas (Fig. 1) has been influenced by the changing dynamics of the Scandinavian Ice Sheet (SIS) and thus records a number of different palaeogeographical settings since the Last Glacial Maximum (Table 1) (Björck 1995; Andrén *et al.* 2015). Some of the events affecting the Skagerrak include, for example, the drainage of the Baltic Ice Lake, the Nedre Glomsjø flood, and the opening of the English Channel and Danish Straits throughout the Holocene (Nordberg 1991; Björck 1995; Jiang *et al.* 1997; Gyllencreutz 2005; Gyllencreutz *et al.* 2006; Rosentau *et al.* 2017; Høgaas *et al.* 2023).

After the initial retreat of the SIS the Baltic Sea Basin developed into the Baltic Ice Lake (BIL) from ~16 cal. ka BP (Björck 1995; Andrén *et al.* 2011; Rosentau *et al.* 2017). The current understanding is that the initial drainage through south-central Sweden (Fig. 1) began at ~13 cal. ka BP, and then paused during the Younger Dryas cold phase (~12.8 cal. ka BP) owing to glacial advance, followed by a rapid (~1–2 years) catastrophic drainage occurring at the end of the Younger Dryas (11.6 cal. ka BP), which lowered the lake level by 25 m with a freshwater discharge of ~7800–9400 km³ (Björck 1995; Andrén *et al.* 2002, 2011; Jakobsson *et al.* 2007; Bennike & Jensen 2013; Stroeven *et al.* 2015; Swärd *et al.* 2015; Muschitiello *et al.* 2016; Rosentau *et al.* 2017).

This drainage event is seen in terrestrial records (e.g. Strömberg 1992; Johnson *et al.* 2010, 2022), but marine records from the Kattegat and Skagerrak are limited (a spike to lighter oxygen isotope compositions in benthic foraminifera at the Swedish west coast interpreted as representing a freshwater flux; Erlenkeuser 1985; Bodén *et al.* 1997; and a sand layer at the Skagen 3 core site interpreted as an erosional deposit; Knudsen *et al.* 1996; Petersen *et al.* 2005). This lack of evidence may partly be due to the large age model uncertainties resulting from (i) issues with the calibration of radiocarbon ages during this time interval (^{14}C plateau and unresolved reservoir age changes; e.g. Björck *et al.* 2003; Guilderson *et al.* 2005; Olsen *et al.* 2009) and (ii) the selection of material that has been dated (e.g. Heier-Nielsen *et al.* 1995).

Another significantly smaller drainage event to affect the Skagerrak is the Glomma drainage event. In SE Norway owing to SIS retreat, several short-lived, ice-dammed lakes formed (e.g. Høgaas *et al.* 2023 and references therein). At ~10.5–10.3 cal. ka BP, ice-margin collapse caused the Nedre Glomsjø glacial lake to release an estimated ~100 km³ of fresh water, flooding the Glomma River valley (Longva & Bakkejord 1990; Longva & Thoresen 1991; Longva 1994; Gyllencreutz 2005; Erbs-Hansen *et al.* 2011b; Høgaas & Longva 2018; Høgaas *et al.* 2023). This outburst affected valleys of SE Norway with an outlet through the Oslo Fjord into the Skagerrak, and resulted in a local rise in sea level during
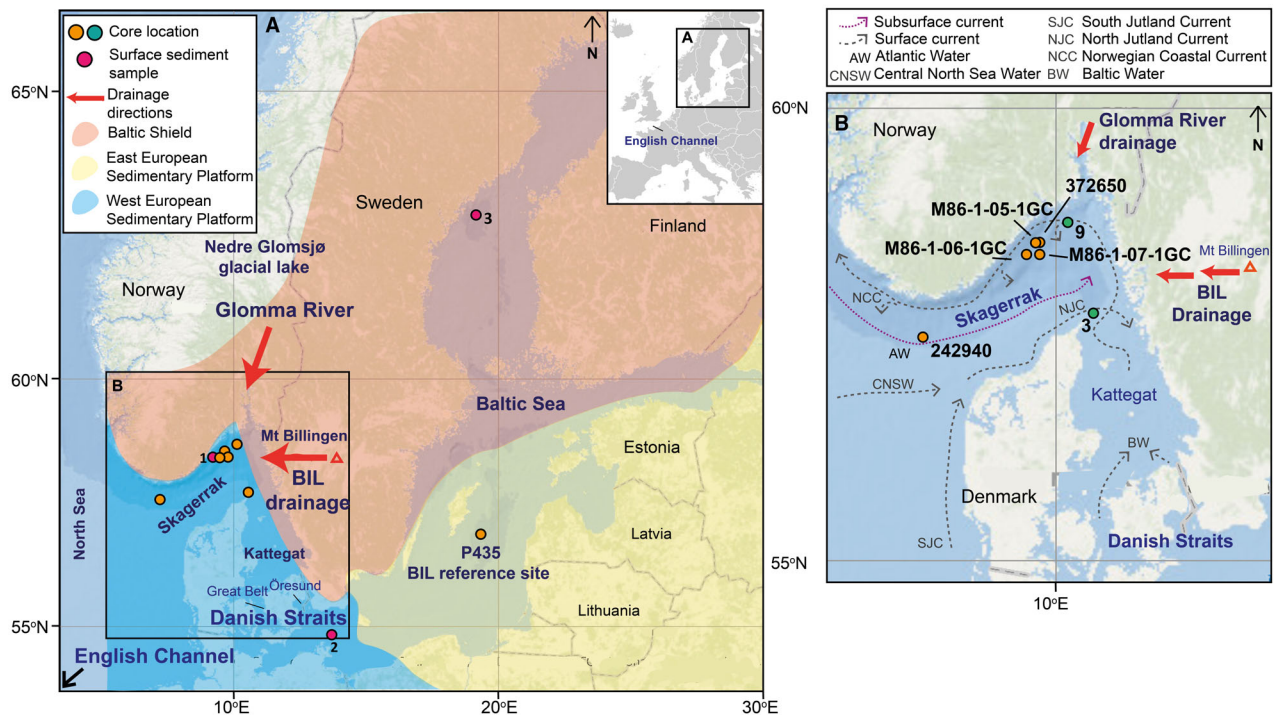
Fig. 1. Map of the Baltic Sea, Kattegat and Skagerrak region showing (A) locations of long cores discussed in the text from the Skagerrak and one from the central Baltic Sea and three surface sediment samples, dominant geology types and the area in south central Sweden around Mt Billingen through which the Baltic Ice Lake (BIL) is thought to have drained, the Danish Straits, English Channel and the approximate location and pathway of the Glomma River drainage event; and (B) the Kattegat and Skagerrak region showing the core sites and also the dominant surface and subsurface currents in the area. The orange circles labelled in the figure are cores that are analysed in this study. The numbered green circles relate to cores from previously published work: 3 = Skagen-3 (Knudsen *et al.* 1996) and 9 = MD99-2286 (Gyllencreutz 2005). The main subsurface current is that of Atlantic Water (AW), and the remaining surface currents include Central North Sea Water (CNSW), the South Jutland Current (SJC) the North Jutland Current (NJC), the Norwegian Coastal Current (NCC) and Baltic Water (BW). The pathways of the BIL drainage and the Glomma drainage event are also marked. Colour white and green maps are from ArcGIS, the grey and white Europe map is from Wikipedia (https://en.wikipedia.org/wiki/File:Europe_blank_map.png), current and subsurface currents are adapted from Gyllencreutz (2005) and geological data from Peucker-Ehrenbrink and Ravizza (1996) and Rosentau *et al.* (2017).

the flood event (Longva & Thoresen 1991; Longva 1994; Høgaas *et al.* 2023). A short-term spike in the input of terrestrial materials and ice-rafted debris recorded in core MD99-2286 (Fig. 1) is considered to record evidence of this drainage (Gyllencreutz 2005; Erbs-Hansen *et al.* 2011b).

Over time, ongoing glacioeustatic sea-level rise led to several periods of opening and enlarging of outlets from the Baltic. The first inflows of marine water into the Baltic Basin have been dated to 9.8 cal. ka BP (Andrén *et al.* 2000; Berglund *et al.* 2005), with the full opening of the Danish straits, such as Öresund and the Great Belt, around ~9.3–8.1 cal. ka BP, allowing greater transfer between the Baltic Sea, Kattegat, Skagerrak and the North Sea (Björck 1995; Berglund *et al.* 2005; Gyllencreutz 2005; Gyllencreutz *et al.* 2006; Björck *et al.* 2008). This, along with the opening of the English Channel ~9.7–7.7 cal. ka BP (recorded in the Skagerrak by distinct changes in foraminifera assemblages and diatoms), begins the transformation of the Skagerrak, Kattegat and Baltic Sea into their modern-day

configurations and circulation patterns (Fig. 1) (Nordberg 1991; Jiang *et al.* 1997; Gyllencreutz 2005; Gyllencreutz *et al.* 2006).

The primary aim of this paper is to improve our understanding of the Lateglacial to Middle Holocene evolution of the Skagerrak region. To achieve this, we use a multiproxy approach from cores across the Skagerrak including the first use of osmium isotopes ($^{187}Os/^{188}Os$) in this area, radiocarbon dating, X-ray fluorescence (XRF) data, sand content, foraminifera species and counts, and $\%C_{37:4}$ biomarkers. A major difficulty in providing detailed reconstructions of the evolution of this region is the development of robust chronologies from palaeorecords. To help address this issue we present a new stratigraphic framework for core correlation across the Skagerrak. This stratigraphic framework is principally based on the appearance of certain key benthic foraminifera species and uses changes in the XRF scanner-derived elemental Ca/K ratio and grain size data. We use these data sets to correlate between cores from multiple locations in the Skagerrak with the

Table 1. Dates of key events to occur in the Skagerrak through the Holocene from previous literature. Noted also are the key ways in which these events are highlighted in this study, discussed in more detail in the text.

Event	^{14}C age (ka BP)	Calibrated age (cal. ka BP)	Calibration	References	Key event features in this study
Final drainage of Baltic Ice Lake		11.62	Varve years with GRIP and NGRIP	Andrén *et al.* (2002) and updated by Stroeven *et al.* (2015)	Potentially high ^{187}Os/^{188}Os, sand, %$C_{37:4}$, *Nonionella labradorica*, *Stainforthia loeblichi* and low Ca/K and carbonate
End of iceberg calving in Skagerrak	10	10.2		Gyllencreutz (2005) (NE Skagerrak)	Fall in ^{187}Os/^{188}Os, sand, %$C_{37:4}$, *N. labradorica*, *S. loeblichi*
		11.6–11.3		van Weering (1982) (SW Skagerrak)	
Glomma drainage event (Nedre Glomsjø outburst)	9.2–8.9	10.5–10.3	IntCal20	Høgaas *et al.* (2023)	Appearance of *Valvulineria*, high %$C_{37:4}$
Opening of English Channel	8.7–7.0	7.7–9.7	IntCal98	e.g. Nordberg (1991), Jiang *et al.* (1997), Gyllencreutz (2005), Gyllencreutz *et al.* (2006)	Appearance of *Hyalinea balthica*, disappearance of *Elphidium excavatum*, drop in %$C_{37:4}$, continued fall in ^{187}Os/^{188}Os
	7.6–7.7	8.6–8.5	Marine 98		
Opening of Danish Straits	8.2–7.5	9.3–8.1	IntCal98	e.g. Björck (1995), Berglund *et al.* (2005), Gyllencreutz *et al.* (2006) and references therein	Appearance of *H. balthica*, disappearance of *E. excavatum*, drop of %$C_{37:4}$, continued fall in ^{187}Os/^{188}Os

aim of developing a robust chronostratigraphic framework that can then be applied to other cores from the region.

Geographical and geological setting of the present-day Skagerrak

The Skagerrak is a large body of water lying south of Norway, west of Sweden and north of Denmark, with a maximum depth of 700 m (Fig. 1) (Nordberg 1991). Circulation in the Skagerrak is described as cyclonic, largely owing to the interactions between the North Atlantic and North Sea inputs and the Baltic Sea outflow, as well as atmospheric patterns (Nordberg 1991; Rodhe & Holt 1996; Gyllencreutz 2005; Larsson *et al.* 2007; Dickens 2013). Present-day detritus derived from the Baltic Sea, the Kattegat and the North Sea is deposited within the Skagerrak largely owing to a reduction in current velocity as the water masses mix (e.g. Rodhe & Holt 1996). As a result, the Skagerrak has a relatively high fine-grained sedimentation rate of up to 1 cm per year (van Weering 1982; van Weering *et al.* 1993; Bøe *et al.* 1996; Gyllencreutz 2005). Connections to the Baltic Sea are through the narrow and shallow Danish/Swedish/German straits. Many of the present-day exchanges between the North Sea and the Baltic Sea must first pass through the connected waterways of the Skagerrak and Kattegat, which together act as a large estuary (Nordberg 1991).

The geological setting of the Skagerrak is largely sedimentary as it mainly lies on the Palaeozoic Western European Sedimentary Platform, consisting mainly of clastic and calcareous rocks, with only the very north of the area in the Baltic Shield (Fig. 1) (Solheim & Grønlie 1983; Rosentau *et al.* 2017). The Baltic Shield is dominated by Precambrian crystalline basement over which the majority of the northern Baltic Sea Basin lies, ranging in age from Late Proterozoic in the south to Late Archaean in the NE over Sweden, Finland and into Russia (Peucker-Ehrenbrink & Ravizza 1996; Rosentau *et al.* 2017).

Material and methods

Sample sites

Three gravity cores, M86-1-05-1GC (M86-5; 8.3 m length; 553 m water depth), M86-1-06-1GC (M86-6; 6.6 m length; 508 m water depth) and M86-1-07-1GC (M86-7; 8.1 m length; 667 m water depth), were obtained from the Skagerrak in 2011 during a RV 'Meteor' cruise (Table 2, Fig. 1). All three cores underwent XRF scanning, while benthic foraminifera counting, sand content determination and rhenium–osmium chemistry were undertaken at determined key intervals most likely to record specific events. Measurements of total inorganic carbon (%) and an alkenone biomarker (%$C_{37:4}$) were made only for core M86-06 (focussing on the interval of the core with decreased Ca/K and increased sand content) owing to logistical constraints on the number of analyses that could be completed.

A fourth core, P435/1-5 GC (P435; 11 m length; 178 m water depth), from the central Baltic (Fig. 1, Table 2; ~60–70 km east of south Gotland Island) was also studied for its rhenium–osmium chemistry to provide insight into the ^{187}Os/^{188}Os ratio for the Baltic Sea during the Baltic Ice Lake stage. This core was collected during the RV 'Poseidon' cruise in 2012. Five samples (chosen from analysis of the full core length) were picked from a short

Table 2. List of core and surface sediment sample localities, including the depth of the cores/depth of the surface sediment.

Type	Sample name	Map label	Depth (cm)	Latitude (°N)	Longitude (°E)	Water depth (m)
Core	M86-1-07-1GC	M86-1-07-1GC	0–810	58°26.370	09°43.530	667
	M86-1-05-1GC	M86-1-05-1GC	0–830	58°29.513	09°34.787	553
	M86-1-06-1GC	M86-1-06-1GC	0–660	58°25.756	09°28.551	508
Core	P435/1-5 GC	P435	720–1000	56°57.954	19°22.210	178
Core	242940	242940	0–500	57°40.52	07°10.00	316
Core	372650	372650	0–527	58°29.76	09°35.91	550
Surface	EMB046/20-2	1	0.5–1	58°31.59	09°29.09	532
Samples	318320-2	2	0	54°49.786	13°39.365	45
(Pink)	P435/10-2 MUC 1AW	3	0	62°52.169	19°2.562	213

section of the core (7.2–10 m) identified sedimentologically to represent the Baltic Ice Lake stage (samples were taken from the lower part of the typical brown glaciolacustrine varved clay; Rosentau *et al.* 2017).

Three other cores located within the Skagerrak (Fig. 1, Table 2) were also examined for their foraminifera contents to aid the comparison and correlation of different, previously studied cores with those in this study. These are: (i) GC242940 from NW Skagerrak (Krossa *et al.* 2015); (ii) GC372650 from central Skagerrak (Dickens 2013); and (iii) MD99-2286 from eastern Skagerrak (Gyllencreutz 2005).

In addition to the sediment cores, three surface sediment samples were collected from the Skagerrak, and the SW and north Baltic Sea (Bothnian Sea) to assess the variability of the $^{187}Os/^{188}Os$ composition along a marine to brackish to relatively freshwater transition (Fig. 1, Table 2).

Foraminifera identification and counts

We identified five key benthic foraminifera species based on earlier studies in the area (e.g. Knudsen *et al.* 1996; Gyllencreutz *et al.* 2006; Erbs-Hansen *et al.* 2011b; Dickens 2013). These are: *Nonionella labradorica*, *Stainforthia loeblichi*, *Elphidium excavatum*, *Valvulineria* spp and *Hyalinea balthica*, which reflect marked environmental changes in the region and aid biostratigraphic correlation between the studied cores (see Table S1, Data S1–S3).

For cores 242940, M86-5, M86-6 and M86-7 we present the absolute abundance (numbers of tests per gram) of the key benthic foraminiferal species to be used as biostratigraphic markers across the Skagerrak. For core 372650 we present the relative abundance of selected species as biostratigraphic markers and also for palaeoenvironmental reconstruction (full foraminiferal counts for 372650 are taken from Dickens 2013).

From core 242940, samples were taken for foraminiferal analysis (on grain size fraction >125 μm) at varying intervals ranging from 10 to 25 cm for the lower sections of the core. For M86-5, M86-6 and M86-7, benthic foraminifera counts were performed on material (grain size fraction >63 μm) taken every 4 cm. Samples from

372650 (Dickens 2013) were taken at a resolution ranging from 4 to 8 cm. Approximately 4 g of sample was soaked in deionized water for several hours to aid disaggregation. Foraminifera were concentrated using 500 and 63 μm mesh sieves and selected species were counted from the dried residue >63 μm. All species were identified and counted to a target count of 300 specimens per sample.

X-ray fluorescence analysis

The semi-quantitative distribution of a range of elements was determined by XRF core scanning (ITRAX XRF Core Scanner, COX; e.g. Croudace *et al.* 2006) at the Leibniz-Institute for Baltic Sea Research Warnemünde (IOW). Core surfaces were cleaned, smoothed, and covered with a thin plastic foil to avoid evaporation during measurements. A Cr tube was used operating at 30 kV and 30 mA with an exposure time of 15 s per step. The step size was 1 mm. Of particular interest were the elements K and Ca, selected for use as a proxy relating to clay minerals, biogenic and terrestrial input (Hebbeln *et al.* 2006; Rothwell & Croudace 2015; Demina *et al.* 2019). The Ca/K ratios for core MD99-2286 were obtained from the PANGAEA database (Erbs-Hansen *et al.* 2011a, b).

Sand content

For cores 242940, 372650, M86-5, M86-6 and M86-7 sediment samples (at 2–4 cm intervals and ~20–30 g) were freeze-dried, weighed, wet sieved at 63 μm grain size, then dried and weighed again to determine the sand content (wt%) at the IOW.

Carbonate and calcite contents

For core M86-6, total inorganic carbon (TIC) was determined (carbonate % = TIC % × 8.33) at ~2 cm intervals using 100 mg of freeze-dried sediment that was diluted with 40% H_3PO_4 and incinerated at 1200 °C on a Multi EA4000 from Analytik Jena at IOW. Relative calcite content downcore changes (presented as counts per second, cps) were determined by X-ray diffraction

(Phillips device, Co Kα-radiation) based on the 3.03 Å calcite reflection.

Biomarker alkenones (%C$_{37:4}$)

To reconstruct the freshwater influence associated with sediment deposition biomarker alkenone %C$_{37:4}$ analyses were conducted for cores M86-6, 372650 and 242940 at the Biomarker Laboratory at the Institute of Geosciences, Kiel University. A sample interval of ~2 cm was used for M86-6 between 570 and 670 cm, for 372650 between 0 and 550 m and for 242940 between 4.6 and 2 m. Long-chained alkenones (C$_{37}$) were extracted from 2–3 g of homogenized bulk sediment using an accelerated solvent extractor (Dionex ASE-200) with a mixture of 9:1 (v/v) of dichloromethane–methanol at 100 °C and 100 bar N$_2$(g) pressure for 20 min. Extracts were cooled to about −20 °C and taken to near dryness by vacuum rotary evaporation (20 °C, 65 mbar). A multidimensional, double gas column chromatography with two Agilent 6890 gas chromatographs was used for C$_{37:2}$, C$_{37:3}$ and C$_{37:4}$ identification and quantification (Etourneau *et al.* 2010), achieved with the addition of an internal standard prior to extraction (cholestane (C$_{37}$H$_{48}$) and hexatriacontane (C$_{36}$H$_{74}$)). The relative proportions were obtained using the peak areas of the two different compounds. The specific proportion of tetra unsaturated C$_{37}$ ketones relative to the sum of alkenones (%C$_{37:4}$) was used. This ratio serves as an indicator of the presence of lower surface salinities in polar and subpolar waters (Rosell-Melé 1998; Rosell-Melé *et al.* 2002; Sicre *et al.* 2002; Bendle *et al.* 2005; Moros *et al.* 2016) and has successfully been used for the reconstruction of Mid to Late Holocene Baltic Sea outflow changes in the study area (Krossa *et al.* 2015).

Rhenium–osmium analysis

Fifty-seven down-core sediment samples from four cores were analysed for rhenium–osmium (Re–Os) abundance (parts per billion, ppb and parts per trillion, ppt, respectively) and isotopic compositions (^{187}Re/^{188}Os and ^{187}Os/^{188}Os) along with the three surface samples (17 from M86-5, 24 from core M86-7, 11 from M86-6, 5 from P435). Each sampled interval records 1 cm of stratigraphy. The Re–Os analytical protocol is based on established methods (Selby & Creaser 2003) and was carried out at Durham University (Durham Geochemistry Centre). Approximately 1 g of dried and powdered sample was sealed into a Carius tube with 8 mL of CrO$_3$ 4 M H$_2$SO$_4$ and a pre-determined amount of tracer solution (enriched in ^{185}Re and ^{190}Os) and heated at 220 °C for 48 h in an oven. The Carius tubes were opened, and a solvent extraction was undertaken using 9 mL of chloroform and back extraction into 3 mL of HBr. Further purification of the Os fraction was achieved using a H$_2$SO$_4$−CrO$_3$−HBr microdistillation.

Purification of the Re fraction was obtained using a 5 M NaOH–acetone extraction, which was then further purified using HCl–HNO$_3$ anion bead chromatography. The Os and Re fractions were loaded into a Thermo-Scientific TRITON mass spectrometer on Pt and Ni filaments, respectively, and analysed using negative thermal ionization mass spectrometry.

The total analytical protocol blanks ($N = 8$) are 19.04±4.67 ppt for Re and 0.08±0.05 ppt for Os, with a ^{187}Os/^{188}Os ratio of 0.27±0.20; 1 SD. To monitor the reproducibility of the Re–Os isotopic analyses over the long term, Re and Os standard solutions are analysed with every sample set. A 50 pg osmium standard solution (Durham Romil Osmium Standard) gives ^{187}Os/^{188}Os values of 0.16080±0.00025 (1 SD, $N = 25$), which is in agreement with proposed values for the solution and the laboratory running average (Luguet *et al.* 2008; Nowell *et al.* 2008; 0.16082±0.0006 1 SD; $N = 816$). The 125 pg rhenium standard solution (Restd) yields ^{185}Re/^{187}Re values of 0.59834±0.00063 (1 SD, $N = 25$), which agrees with the laboratory running average (0.59861±0.0015 1 SD; $N = 720$).

Radiocarbon dating

Thirty-eight samples were obtained for radiocarbon dating, eight from M86-5, seven from M86-7, seven from M86-6, six from 372650 and 10 from 242940 (Table S1). Analyses were on mixed benthic foraminifera species, monospecific foraminifera or mollusc shells. Analysis was undertaken at the Poznań Radiocarbon Laboratory in Poland, the Laboratory of Ion Beam Physics at Eidgenössische Technische Hochschule in Zürich, Switzerland and the Leibniz Laboratory for Age Determinations and Isotope Research at the University of Kiel using accelerator mass spectrometry (AMS).

In cases where calibrated dates are used, the radiocarbon dates were calibrated using Calib 8.2 using the Marine20 calibration curve and a local reservoir correction (ΔR) of −166±59 based on an average of five sites (sites 76, 82, 84, 85 and 86) in the Skagerrak and Kattegat on the Calib marine reservoir correction database (Mangerud 1972; Mangerud & Gulliksen 1975; Heier-Nielsen *et al.* 1995; CALIB rev. 8 *et al.* 1993). This reservoir correction was applied to all dates throughout the core regardless of freshwater input changes.

Results

Foraminifera identification and counts

The five main benthic foraminifera species *N. labradorica*, *S. loeblichi*, *E. excavatum*, *Valvulineria* spp. and *H. balthica* (Fig. 2) were analysed across all six Skagerrak cores (MD99-2286 is described in Erbs-Hansen *et al.* 2011b). Three other species (*Buccella frigida*, *Nonionella iridea* and *Pullenia osloensis*: Fig. 3) from
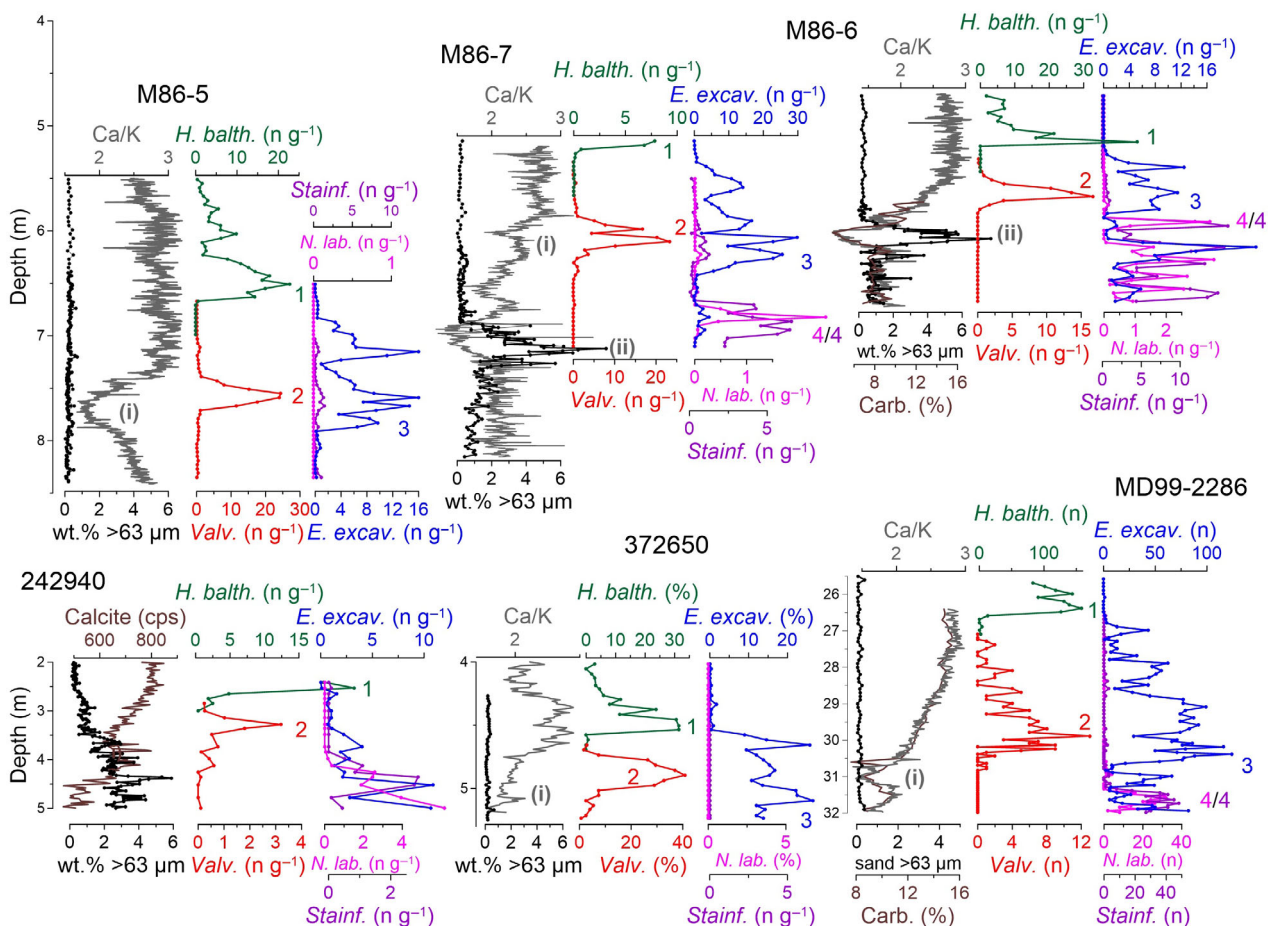
Fig. 2. Sand content (wt% <63 μm), Ca/K, and benthic foraminifera species *Hyalinea balthica*, *Elphidium excavatum*, *Valvulineria* spp., *Stainforthia loeblichi*, and *Nonionella labradorica* against depth (m) for Skagerrak cores M86-5, M86-7, M86-6, 242940, 372650 and MD99-2286 (from Erbs-Hansen *et al.* 2011a, b). Carbonate (%) and calcite (cps) are also shown for M86-6 and 242940, respectively. Labels (i) and (ii) show tie points in Ca/K ratio used to correlate between cores. Numbers 1–4 show tie points between the peaks in benthic foraminifera used to correlate between cores.

372650 (Dickens 2013) are also discussed here. Several similarities in the increase and decline of certain species can be seen through all the Skagerrak cores (numbered 1–4, Fig. 2) and are described in more detail below. These variations are key to developing the core correlations (Data S1). Owing to the differences in the way that the foraminifera have been counted (on different size fractions) between the different cores, the overall trends of species are described below, rather than absolute values.

A large and sudden peak in both the species *H. balthica* (no. 1 in Fig. 2) and *Valvulineria* (no. 2 in Fig. 2), respectively, is recorded across all cores in M86-5 (at ~6.5 and ~7.6 m), M86-7 (at ~5.1 and ~6.1 m), M86-6 (at 5.1 and ~5.6 m), 242940 (at ~2.6 and ~3.4 m), 372650 (at ~4.5 and ~4.9 m) and MD99-2286 (at ~26.5 and ~30.5 m), compared with relatively low or zero abundances across the rest of the counted intervals (Fig. 2).

The species *E. excavatum* is more variable across all cores. However, a large and broad peak (no. 3 in Fig. 2) is

comparable across all Skagerrak cores including in M86-5 (~7.8 m), M86-7 (~6.2 m), M86-6 (~5.8 m), 242940 (~4 m), 372650 (~5.1 m) and MD99-2286 (~30.5 m).

In the lower sections of cores M86-7, M86-6, 242940 and MD99-2286 levels of the species *N. labradorica* and *S. loeblichi* (Fig. 2) fluctuate before a sudden decrease to very low/zero values through the rest of the counted sections. A separate, traceable peak (no. 4 on Fig. 2) is clearly seen in the high-resolution cores M86-7 (~6.8 m) and M86-6 (~6 m) and in Skagen 3 (~115 m; Data S3) on top of a marked sand layer. MD99-2286 (Fig. 2) records a *N. labradorica* and *S. loeblichi* spike (Fig. 2 at ~31.5 m) but not a sand layer. As cores M86-5 and 372650 do not reach far back in time, there are very few to zero counts of the species *N. labradorica* and *S. loeblichi* recorded across the measured intervals (Fig. 2).

In 372650, levels of *B. frigida* begin at a peak of ~40% and then drop to close to 0% at ~5 m where levels remain low (Fig. 3). *Pullenia osloensis* levels fluctuate between 8 and 16% between ~5.3 and 4.5 m and decrease from this
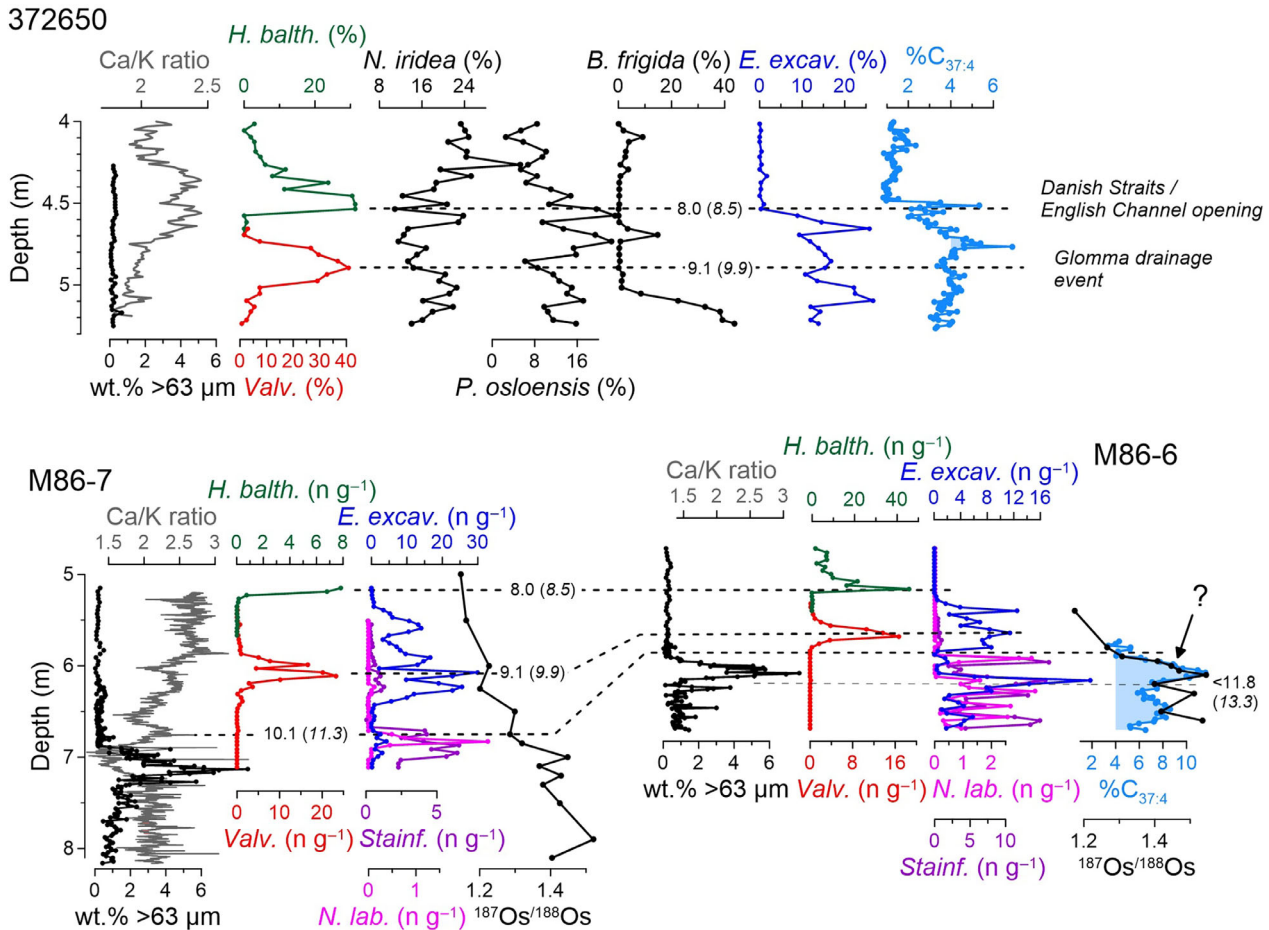
Fig. 3. Sand content (wt% >63 μm), Ca/K ratio and benthic foraminifera species *Hyalinea balthica, Valvulineria* spp, and *Elphidium excavatum* against depth (m) for cores 372650, M86-7 and M86-6. Core 372650 also includes the benthic foraminifera species *Buccella frigida, Nonionella iridea* and *Pullenia osloensis* and %C_{37:4} biomarker data. Cores M86-7 and M86-6 also include benthic foraminifera species *Stainforthia loeblichi*, and *Nonionella labradorica* and ^{187}Os/^{188}Os ratios. Core M86-6 further includes %C_{37:4} biomarker data. Dashed lines show the age tie points correlated between cores. Dates are given in ^{14}C ka BP followed by cal. ka BP in brackets. The main events discussed in the text are labelled.

point to <8%. *Nonionella iridea* remains relatively high over the counted interval, fluctuating mainly between ~10 and 24%.

Sand analysis and sedimentology

Relatively homogenous brownish, silty, clayey sediments, which are interrupted by more sandy sections as described below, characterize the sedimentology of the Skagerrak cores. The central Baltic P435 core samples are taken from the lower part of a section of glacial, brown, varved, clays that were probably deposited during the Baltic Ice Lake stage of the Baltic Seas history (e.g. Rosentau *et al.* 2017). The three surface samples analysed are a mix of sandy, muddy to clayey sediments with occasional shelly detritus and larger clasts (which were removed prior to powdering).

Cores M86-6 and M86-7 have a sand content (wt% >63 μm) of <2% for most of the measured interval, except for a large peak to ~8% comparable between the

two cores at depths of 5.9–6.2 m in M86-6 and 6.8–7.4 m in M86-7 (Fig. 2). In core 242940, the sand content overall gradually decreases from ~4 to <1% between 5 and 2 m, with a peak to 6% at ~4.4 m (Fig. 2). In contrast cores M86-5, MD99-2286 (Gyllencreutz 2005; Hebbeln *et al.* 2006) and 372650 are characterized by <1% sand in the analysed intervals (Fig. 2).

XRF and carbonate content

From the range of elemental data obtained by XRF scanning, the ratio of Ca/K is presented. This ratio is used as Ca is a good reflection of calcite/carbonate contents measured in some of the cores (for core correlation purposes, see Data S1–S3; e.g. Hebbeln *et al.* 2006; Demina *et al.* 2019) and K shows minimal variation over the measured intervals.

All cores where the Ca/K is recorded show relatively consistent (M86-5) or overall increasing (M86-7, M86-6, 372650 and MD99-2286) Ca/K ratios from the deepest to

the shallowest sections, that are interrupted by one or two dips in values (Fig. 2). This is mirrored by the calcite and carbonate values in 242940 and MD99-2286, respectively (Fig. 2). Cores M86-5, M86-7, 372650 and MD99-2286 all show a dip in the Ca/K ratio of ~0.5–1.5 comparable between the cores (letter (i) on Fig. 2) centred at depths of ~7.7, 6.0, 5.0 and 31 m, respectively. In core MD99-2286 this dip in Ca/K is accompanied by a dip in carbonate of ~2% at the same depth, and in 242940 this dip is represented by a fall in calcite cps ~3.5 m (letter (i) on Fig. 2). Cores M86-7 and M86-6 also show a second, deeper, dip in Ca/K of around 1–1.5 (letter (ii) on Fig. 2) centred at ~7.0 and 6.0 m, respectively. The carbonate content in M86-6 mirrors this dip in Ca/K, decreasing by ~4% at 6.0 m. In core 242940 this is represented by a drop in calcite cps at ~5 m. Cores M86-5, 372650 and MD99-2286 do not record this second dip (Fig. 2), as with the sand peak described above it is likely that these cores do not go deep enough to recover this horizon.

Rhenium–osmium

Given the age of the analysed sediment ($\sim\leq14$ ka) and relatively low Re abundance, any age correction for the radiogenic ^{187}Os ingrowth from ^{187}Re decay since sediment deposition is less than that of the individual sample ^{187}Os/^{188}Os 2SE uncertainty and also the sample reproducibility of in-house reference samples (e.g. Nowell *et al.* 2008; Du Vivier *et al.* 2014; Sproson *et al.* 2022). As such, age-corrected ^{187}Os/^{188}Os values are not presented.

All three M86 Skagerrak cores show similar trends in the Re–Os data. In M86-05 the Re content is very similar (1.07–1.66 ppb, parts per billion), except that between 8 and 7 m (3.63 ppb) the total Os increases steadily from the core bottom (74 ppt, parts per trillion) to the top (140 ppt) and the ^{187}Os/^{188}Os values show an abrupt decrease from 7.8 to 7.5 m (1.31–1.20), and then remain relatively similar (1.17–

1.12) (Fig. 4). For M86-06, Re–Os measurements were only carried out in the lower part of the core. The Re concentrations are 1–2 ppb except for two at 5.95 m (2.83 ppb) and 6.30 m (3.36 ppb). The total Os varies between 63.6 and 85.1 ppt and generally increases between 6.5 and 5.4 m. The ^{187}Os/^{188}Os ratio shows an abrupt decrease (1.6–1.2) over the same depth interval (Fig. 4). Finally, in M86-07 Re abundances increase from the core bottom (0.77 ppb) to the core top (1.74 ppb) except for at 6.75 m (3.59 ppb) and 3 m (5.09 ppb). The total Os also increases from the core bottom (70 ppt) to the core top (140 ppt). The ^{187}Os/^{188}Os ratio shows an overall decreasing trend from 1.4–1.5 at the core base to 1.1 at the core top, with a sharp decrease between 7 and 6.5 m (Fig. 4).

In core P435 Re concentrations range between 0.43 and 0.67 ppb, with the total Os concentrations varying between 50.6 and 66.5 ppt. The ^{187}Os/^{188}Os values range between 2.67 and 2.25 (Table 3). Further, the surface sample Re and total Os abundances vary between 0.8 and 3.5 ppb, and between 61 and 166 ppt, respectively (Table 3). The ^{187}Os/^{188}Os values are 1.01 for the Skagerrak sample, 1.67 for the SW Baltic Sea sample and 2.24 for the northern Baltic Sea sample (labels 1–3 respectively; Fig. 1A).

Biomarkers (core M86-6, 372650 and 242940 only)

M86-6 records two peaks in %$C_{37:4}$ between 6.7–6.4 m (8.6%) and 6.4–5.9 m (11%), decreasing to 4–6% in the troughs (Fig. 3). The %$C_{37:4}$ in 372650 gradually increases between 5.3 and 5 m from around 3.5 to 4.5%. This is followed by a peak in values to ~7% centred at ~4.8 m. Values then decrease to 2.5% at 4.6 m before another peak in values to 5.5% at 4.5 m, before values quickly decrease to between 1 and 2% between 4.5 and 4 m (Fig. 3). In 242940 the %$C_{37:4}$ overall gradually decreases up core from ~4 to 0.5%. A peak of ~3% occurs at ~3.0 m.

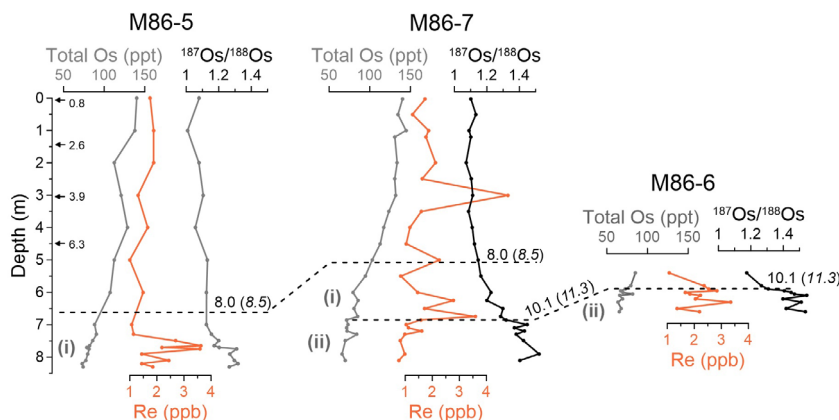*Fig. 4.* Total Os (ppt – parts per trillion), Re (ppb – parts per billion) and ^{187}Os/^{188}Os ratio for cores M86-5, M86-7 and M86-6 against depth (m). Dashed lines show the age tie points correlated between cores. Dates are given in ^{14}C ka BP followed by cal. ka BP in brackets.

Table 3. Re, Os and ^{187}Os/^{188}Os data for the five central Baltic Basin core samples over the Baltic Ice Lake interval and the three Baltic Basin present-day surface samples. Units ppt = parts per trillion, ppb = parts per billion.

Map label	Sample	Depth (cm)	Re (ppb)	Re ±	Os (ppt)	Os ±	^{187}Os/^{188}Os	^{187}Os/^{188}Os ±
P435	P435/1-5GC 720 cm	720	0.4	0.0	65.5	0.6	2.67	0.03
	P435/1-5GC 8 m	800	0.4	0.0	54.4	0.4	2.54	0.03
	P435/1-5GC 880 cm	880	0.6	0.0	53.3	0.4	2.25	0.03
	P435/1-5GC 940 cm	940	0.6	0.0	51.5	0.4	2.42	0.03
	P435/1-5 10 m	1000	0.7	0.0	50.6	0.4	2.43	0.03
1	EMB046/20-2	0.5–1	0.8	0.0	165.5	0.8	1.01	0.01
2	318320-2	0	3.5	0.0	61.4	0.3	1.67	0.01
3	P435/10-2 MUC 1AW	0	0.9	0.0	117.1	1.0	2.24	0.03

Radiocarbon dating

Overall, 38 radiocarbon dates were recorded across the M86 cores 372650 and 242940 (Table S1) (MD99-2286 dates from Gyllencreutz 2005). A synopsis of how these dates were used to correlate between the cores and produce the age estimates used in this study is detailed briefly in the section 'Core correlation based on a biostratigraphic and lithostratigraphic approach' below.

The five main correlation age tie points used in Fig. 4 are dated to 8.0 ^{14}C ka BP (8.5 cal. ka BP), 9.1 ^{14}C ka BP (9.9 cal. ka BP), 9.8 ^{14}C ka BP (10.9 cal. ka BP), 10.1 ^{14}C ka BP (11.3 cal. ka BP) and 11.8 ^{14}C ka BP (<13.3 cal. ka BP; Table 4).

Discussion

Using the combined multiproxy data set described above, we have identified three 'events' in the Skagerrak dated to between an age bracket of ~11.8–10.1 ^{14}C ka BP (~13.3–11.3 cal. ka BP), and at 9.1 ^{14}C ka BP (9.9 cal. ka BP) and 8.0 ^{14}C ka BP (8.5 cal. ka BP). Below, we first outline the development of our new chronostratigraphic framework combining the appearance of key benthic foraminifera, XRF scanning and grain size data with carefully selected radiocarbon dates. This is then used throughout the rest of the discussion. We then outline the use of osmium isotopes as a freshwater proxy before discussing the above-mentioned events in more detail.

Core correlation based on a biostratigraphic and lithostratigraphic approach

A detailed examination of the core correlation and chronology used in the discussion below can be found in Table S1 and Data S1–S4, including detailed methodology and accompanying figures. In brief, we use common peaks ('features') in certain species of benthic foraminifera, carbonate/calcite content and Ca/K across the analysed cores to correlate. These features are labelled in Fig. 2 and represent: 1, the appearance of *H. balthica*; 2, the spike in *Valvulineria* spp.; 3, the *E. excavatum* increase immediately below 2; 4, the *N. labradorica* and *S. loeblichi* spike on top of sand peak; and ii, Ca/K and carbonate lows and sand peak (more detail is provided in Table S1 and Data S1–S4). As pointed out by Heier-Nielsen *et al.* (1995), the use of benthic foraminifera for dating in the Skagerrak is difficult owing to mixed assemblages and also sediment reworking causing age reversals (for example, this can be seen in core M86-7 at 710 cm; Table S1). Therefore, for the assignment of uncalibrated ^{14}C ages to the identified features we used the following approach: (i) ^{14}C ages of molluscs are most reliable; (ii) monospecific benthic foraminifera dates are useful at depths where the respective species appears *in-situ* and is not present lower down in the core dated or at very low numbers; and (iii) foraminiferal dates in low sedimentation rate cores (specifically in 242940) are considered more reliable than cores with higher sedimentation rates. The ages from mixed benthic foraminifera, while less precise, can be used to provide maximum ages.

Table 4. Calibrated radiocarbon ages for key points listed in Data S1 and Figs 2–4 using the Marine20 calibration curve in Calib 8.2.

^{14}C age (years BP)	Reservoir ΔR (years)	1σ calibration (cal. a BP)	2σ calibration (cal. a BP)	Median probability (cal. a BP)	Corresponding feature (see Figs 2, 4, Table S1, Data S1–S4)
8010±50	−166±59	8370–8580	8280–8750	8490	Foraminiferal feature 1 – appearance of *Hyalinea balthica*
9125±50	−166±59	9770–10 070	9620–10 170	9910	Foraminiferal feature 2 – spike in *Valvulineria* spp.
9810±50	−166±59	10 710–11 010	10 580–11 120	10 850	Foraminiferal feature 3 – *Elphidium excavatum* increase
10 110±60	−166±59	11 120–11 380	11 010–11 590	11 250	Foraminiferal feature 4 – *Nonionella labradorica* and *Stainforthia loeblichi* spike, on top of sand layer
11 340±80	−166±59*	12 720–12 950	12 640–13 040	<12 840	Youngest dates obtained close to base of sand peak in M86-7 and M86-6
11 810±60	−166±59*	13 180–13 400	13 080–13 510	<13 300	

*Reservoir ΔR probably higher owing to increased freshwater input.

Radiocarbon calibration

Based on the approach presented above we are able to provide well-constrained age control for the identified marked environmental changes (Figs 2–4). However, we cannot present a composite age model/master chronology for the entire deglacial and Early Holocene time interval as the number of reliable AMS ^{14}C dates in any individual core to provide a precise age model is too low. Sedimentation rate changes probably linked to the marked environmental shifts which stem partly from massive meltwater outbursts are not well constrained, adding further difficulty in developing a full age model. In future studies, this might be possible. However, currently there are still issues relating to radiocarbon dating in the Skagerrak, including unknown and variable reservoir ages and the existence of radiocarbon plateaus in the Early Holocene (e.g. Björck *et al.* 2003; Guilderson *et al.* 2005), further hampering the reliability of developing calibrated age models. We are also aware that owing to increased freshwater inputs in the older sections of the cores, the reservoir age would change over these intervals and hence the calibrated ages in these sections are probably too old (e.g. Olsen *et al.* 2009). We have therefore only calibrated the dates used in the tie points discussed above and use them as general markers rather than developing an age–depth model (see Data S1 for further details).

Use of osmium isotopes as a freshwater input proxy

This study uses sediment ^{187}Os/^{188}Os analysis to infer the water ^{187}Os/^{188}Os composition of the Skagerrak and in the Baltic Basin at the time of sediment deposition (Ravizza & Turekian 1989; Cohen *et al.* 1999). The ^{187}Os/^{188}Os proxy can differentiate changes in the environment owing to the relatively short residence time of osmium in the oceans (1–50 ka, several studies <10 ka; Sharma *et al.* 1997; Oxburgh 1998, 2001; Levasseur *et al.* 1999; Peucker-Ehrenbrink & Ravizza 2012; Rooney *et al.* 2016; Ownsworth *et al.* 2023). The average ^{187}Os/^{188}Os of present-day oxic seawater is relatively stable across the global oceans at 1.060±0.005, with spatial and temporal variations reflecting local influences on ocean chemistry, especially in more isolated/restricted seawater basins (Sharma *et al.* 1997; Levasseur 1998; Burton *et al.* 1999, 2010; Peucker-Ehrenbrink & Ravizza 2000, 2012; Cohen 2004; Chen *et al.* 2009; Paquay & Ravizza 2012; Gannoun & Burton 2014; Kuroda *et al.* 2016; Rooney *et al.* 2016; Ownsworth *et al.* 2023).

Previous research has shown runoff from Precambrian crystalline basement (Baltic Shield) to have a highly radiogenic ^{187}Os/^{188}Os signature of ~3.6–7.9 (Peucker-Ehrenbrink & Ravizza 1996). Freshwater runoff from the catchment then delivers this radiogenic signature into the Baltic Basin. This is demonstrated by present-day

sediment ^{187}Os/^{188}Os compositions. Surface sediment sample 1 from the Skagerrak has a ^{187}Os/^{188}Os ratio of 1.01 (Fig. 1, Table 3), close to open ocean values (1.06). Sample 2 from the SW Baltic Sea has a ^{187}Os/^{188}Os ratio of 1.67 representing a decreased marine influence, shown by decreasing salinity values of 30–15 PSU in the Skagerrak through to 8 PSU in the southern Baltic Sea (Jiang *et al.* 1997; Ducrotoy & Elliott 2008). Sample 3 from the north Baltic Sea, almost fresh water at 5 PSU, is much more radiogenic with a ^{187}Os/^{188}Os of 2.24 owing to an increased influence of radiogenic runoff from the Baltic Shield. Therefore, there is a clear difference between the ^{187}Os/^{188}Os of a Skagerrak marine signature and a restricted Baltic Sea Basin with high influence from the Baltic Shield.

During the freshwater Baltic Ice Lake stage, the Baltic Basin was isolated from marine influence, and therefore a radiogenic ^{187}Os/^{188}Os signature is expected to characterize the basin during these times, similar to the present-day north Baltic Sea sample (sample 3; ~5 PSU) at 2.24. Indeed, this point is clearly supported by the sediments analysed from core P435 (Fig. 1). The ^{187}Os/^{188}Os values within the clay recording deposition during the Baltic Ice Lake stage are highly radiogenic (2.25–2.67; Table 3), reflecting the radiogenic ^{187}Os/^{188}Os derived from runoff from the Precambrian Baltic Shield, without input from the North Sea. The ^{187}Os/^{188}Os of the Baltic Ice Lake phase (2.25–2.67) is very different from that of the Late Pleistocene and Holocene global ocean (~1; Paquay & Ravizza 2012; Rooney *et al.* 2016). Based on this the ^{187}Os/^{188}Os ratio has the potential to record changes in the influence of freshwater inputs from the Baltic Shield/Baltic Sea Basin and open marine inputs into the Skagerrak.

Earliest Holocene palaeoceanography of the Skagerrak

This study presents evidence from several Skagerrak cores showing an 'event-like' feature characterized by an increase in sand content similar to the coarse sand layer in the Skagen-3 core (Knudsen *et al.* 1996; Data S4), and an increase in freshwater biomarkers and osmium isotopes. The evidence of this event and potential explanations are discussed below.

Based on the chronology developed in this study from the combination of biostratigraphic markers and radiocarbon dates, the oldest sequence recovered is preserved in cores M86-6 and M86-7, both dating back >12.8 ^{14}C ka BP (>14.6 cal. ka BP; Table 4; however, an age plateau/hiatus is potentially apparent at >~738 cm depth, see Table S1 M86-7). In the deepest recorded section (>11.3 cal. ka BP) of M86-7 and M86-6, the ^{187}Os/^{188}Os compositions are more radiogenic (1.2–1.5; Figs 3, 4, Table 4) than contemporaneous and present-day average open marine values (~1; Table 3; Sharma *et al.* 1997; Levasseur 1998; Burton *et al.* 1999; Peucker-Ehrenbrink & Ravizza 2000; Cohen 2004; Paquay &

Ravizza 2012; Rooney *et al.* 2016; this study). The values are, however, less radiogenic than the ^{187}Os/^{188}Os compositions of the Baltic Ice Lake waters (~2.2–2.7) inferred from core sediments deposited in the central Baltic during the Baltic Ice Lake stage and the present-day surface sample from within the Baltic (2.24; Table 3). This indicates a mixing of two different sources – marine waters from the North Sea and waters drained from a more radiogenic continental setting influenced by the radiogenic geologies of the Baltic Shield. This could be from glacial meltwater flux from the retreating SIS across Sweden and Norway over the Baltic Shield to the north of the Skagerrak or could potentially be from freshwater drainage/outflow from the Baltic Ice Lake. This shows that the ^{187}Os/^{188}Os values from sediment cores are effective in recording inputs of more radiogenic freshwater into the Skagerrak but cannot alone distinguish between different freshwater sources from the region.

Further evidence of a freshwater influence during this period is provided by the %$C_{37:4}$ biomarkers and foraminifera species. The biomarker proxy (%$C_{37:4}$) records the influences of freshwater, being an indicator of lower surface ocean salinities (Rosell-Melé 1998; Rosell-Melé *et al.* 2002; Sicre *et al.* 2002; Bendle *et al.* 2005; Moros *et al.* 2016), and has successfully been used to show changes in the outflow from the Baltic Sea into the Kattegat during the Middle to Late Holocene (Krossa *et al.* 2015). Core M86-6 records two peaks in %$C_{37:4}$ biomarkers (Fig. 3) between ~6.7 and 6.3 m, and between ~6.3 and 5.9 m. The peak in %$C_{37:4}$ between 6.3 and 5.9 m correlates with the more radiogenic ^{187}Os/^{188}Os and the subsequent drop in %$C_{37:4}$ is coincident with the decline in ^{187}Os/^{188}Os (Figs 3, 4). The peak in %$C_{37:4}$ therefore suggests increased freshwater input into the Skagerrak during this time, followed by a decline in freshwater input to ~11.3 cal. ka BP. In cores M86-7 and M86-6, the sediments older than 11.3 cal. ka BP contain higher abundances of the foraminifera species *N. labradorica* and *S. loeblichi* compared with the shallower (younger) sections of the cores, with abundances dropping suddenly around 11.3 cal. ka BP (Fig. 3). This decline is also coincident with the decline in %$C_{37:4}$ and ^{187}Os/^{188}Os (Fig. 3). There are also more variable levels of *E. excavatum* in this section. Both *N. labradorica* and *S. loeblichi* are indicative of relatively cold conditions, commonly found in ice-distal environments associated with seasonal sea-ice cover, and *E. excavatum* is also a relatively cold, boreal indicator species (Jennings & Helgadottir 1994; Knudsen *et al.* 1996; Hald & Korsun 1997; Korsun & Hald 1998; Erbs-Hansen *et al.* 2011b). These faunal shifts suggest cooling conditions during this interval associated with significant cold meltwater flux.

Coincident with increasing freshwater influence in the Skagerrak, cores M86-7 and M86-6 also record an increase in the >63 μm fraction (sand content) and a dip in the Ca/K ratio (drop in Ca; feature ii) (Fig. 2). The increase in the >63 μm fraction implies an increase in detritus/sediment delivery to the core sites alongside the increase in freshwater. The dip in Ca/K owing to a drop in Ca could be linked to a change in productivity and biogenic production and/or increased clay input (e.g. Gyllencreutz 2005; Rothwell & Croudace 2015; Demina *et al.* 2019).

One explanation for the source of radiogenic freshwater and grain size increase recorded in this study between the age <13.3 and 11.3 cal. ka BP could be delivery via iceberg rafting or glacial meltwater from the retreating SIS over the Baltic Shield of southern Sweden and Norway. Iceberg calving is dated to have ended between ~11.6 and 11.3 cal. ka BP in the SW Skagerrak (van Weering 1982) and around 10.2 cal. ka BP in the NE Skagerrak (Gyllencreutz 2005), which in general coincides with the drop to less radiogenic ^{187}Os/^{188}Os values, lower %$C_{37:4}$ values and a finer grain size (Fig. 3). The movement of the meltwater may also have resulted in some remobilization of sediments from previously deposited sand-rich sediments in other parts of the Skagerrak and surrounding areas (Jansen *et al.* 1979; EMODnet 2023).

The final drainage of the Baltic Ice Lake is also dated to occur within the timeframe of this 'event'. The final catastrophic drainage of the BIL occurred at 11.6 cal. ka BP, lasting for ~1–2 years and lowering the lake level by 25 m (Table 1) (e.g. Björck 1995; Andrén *et al.* 2002; Jakobsson *et al.* 2007; Stroeven *et al.* 2015). Evidence of this drainage in the Skagerrak is limited and appears ambitious given the known age calibration uncertainties. A medium to coarse sand layer is also recorded in the Skagen-3 core and is argued to record the BIL drainage (Knudsen *et al.* 1996; Petersen *et al.* 2005) (Fig. 1B). In this study we are only able to give much larger bracketed timeframes (<13.3–11.3 cal. ka BP). Further, our data show an increase in freshwater over the potential interval, which makes predicting reservoir age corrections even more complicated (e.g. Olsen *et al.* 2009). Specifically, our age for the beginning of the freshwater/sand layer event therefore appears too old. Knudsen *et al.* (1996) report radiocarbon dates through the sand unit from Skagen-3 ranging from 10 230±125 ^{14}C BP (11.4 cal. ka BP) towards the top to 10 850±110 ^{14}C BP (12.3 cal. ka BP – probably too old an estimate when keeping in mind reservoir age changes and the possibility of re-working of dated material in the sand layer) at the peak. The similar age estimates of the Skagen-3, M86-6 and M86-7 sand layers highlight the possibility that they may be contemporaneous. The outburst of fresh water from the BIL and potential iceberg output from the ice-margin break-up (e.g. around Timmersdala and Klyftamon; Johnson *et al.* 2022) in theory could help explain the increased freshwater signals and coarser grain size seen in M86-6 and M86-7. However, it has also been noted that the sediment supply carried by the drainage waters may have been limited owing to a short transport distance over land (~20 km) (Johnson *et al.* 2022), which would

impact how far the sediment would disperse. Further work is needed to provide clearer evidence of the wider geographical extent of the sedimentological signal of this drainage event. This is outside the scope of this study as, unfortunately, we do not have enough data or a suitably constrained age model to correlate such a short-lived event with any certainty.

In summary, between <13.3 and 11.3 cal. ka BP both cores M86-6 and M86-7 show a peak in sand content and $\%C_{37:4}$, and a decrease in Ca/K with generally high levels of the relatively cold-water foraminifera species *N. labradorica* and *S. loeblichi* and more radiogenic $^{187}Os/^{188}Os$ values (Fig. 3). All of these data together suggest an increased input of cold, radiogenic freshwater and increased sediment delivery. This could be due to increased iceberg discharge and meltwater input from the retreating SIS which could also have remobilized previously deposited sand-rich layers. A potential contribution may also have come from the drainage of the BIL which occurred during this time interval (11.6 cal. ka BP).

Early Holocene palaeoceanography and the Glomma drainage event

Post 11.3 cal. ka BP $^{187}Os/^{188}Os$ values continue to decrease; however, the composition remains slightly more radiogenic (~1.1–1.3) than the open ocean value (~1; Figs 3, 4). This may suggest that this region of the Skagerrak is still receiving some radiogenic osmium-enriched freshwater input.

During this time, the abundance of *N. labradorica* and *S. loeblichi* has significantly decreased, indicating an amelioration in conditions and a shift to more ice-distal/boreal environmental conditions and all the studied cores record continued variability in *E. excavatum*. The basal sequence identified from 372650 corresponds to this transition, with a fauna dominated by *B. frigida* with relatively high abundances of *E. excavatum* and *N. iridea* (Fig. 3). These species are known to be characteristic of arctic to sub-arctic conditions (Knudsen 1984; Hald & Korsun 1997) and are common around the Greenland margins at the present day (e.g. Lloyd 2006; Jennings *et al.* 2020). This indicates continued relatively cold oceanographic conditions during the transition to the Early Holocene. All Skagerrak cores also record a significant peak in the foraminifera species *Valvulineria* spp, corresponding to an age of 9.9 cal. ka BP (Figs 2, 3, Table 4). Species of *Valvulineria* are commonly found associated with delivery of organic material and clay deposition, often with a significant fluvial flux sometimes leading to increased stratification or even eutrophication (Frezza *et al.* 2005; Morigi *et al.* 2005; Mojtahid *et al.* 2010). Therefore, this indicates a regional episode of increased organic matter delivery, most likely through a short-term increased freshwater flux into the Skagerrak. The most likely

explanation for this is in response to the Glomma drainage event via Oslo Fjord dated to ~10.5–10.3 cal. ka BP (Table 1), which released an estimated ~100 km³ of fresh water into the Skagerrak (Longva & Bakkejord 1990; Longva & Thoresen 1991; Longva 1994; Gyllencreutz 2005; Erbs-Hansen *et al.* 2011b; Høgaas & Longva 2018; Høgaas *et al.* 2023). From 372650 it can also be seen that the $\%C_{37:4}$ levels are still relatively high (~3–4%), indicating a continued freshwater flux, although not as high as the deeper recorded core section in M86-6 (~11%; Fig. 3). This may reflect the fact that the Glomma drainage event is a relatively small event. There is no specific peak in $\%C_{37:4}$ at the same time as the spike in *Valvulineria* spp.; however, a peak in $\%C_{37:4}$ does occur at ~4.7 m, which might be partly in response to the input of freshwater from the Glomma event. Further, no spike in $^{187}Os/^{188}Os$ appears to be recorded in cores M86-5 and M86-7 (Fig. 4), which may be due to a lower sample resolution and/or to the freshwater continental signal becoming too weak/diluted before it reaches the core sites.

Early to Middle Holocene palaeoceanography: development of a modern-like circulation system

The spike in *Valvulineria* at 9.9 cal. ka BP is relatively short-lived in all cores presented here and abundances abruptly decrease, indeed virtually disappearing in most cores (Figs 2, 3). During this period the fauna in all cores continues to be characterized by relatively high abundances of *E. excavatum* with *N. iridea* also continuing to be abundant in core 372650. This indicates continued relatively cold, sub-arctic to boreal oceanographic conditions through to 8.5 cal. ka BP. At this point, there is a significant shift in benthic foraminiferal fauna in all cores. This is characterized by the appearance and abrupt increase in relative abundance of *H. balthica* from ~8.5 cal. ka BP. *Hyalinea balthica* is common at the present day in the Skagerrak, found associated with relatively high concentrations of organic carbon (Qvale & van Weering 1985). This species is also present in the North Sea today, particularly common in well-stratified areas with Atlantic Water at the sea floor, increased organic carbon concentration and associated lowered oxygen concentration (Klitgaard-Kristensen *et al.* 2002). The abrupt increase in abundance of *H. balthica* marks the onset of a modern-like oceanographic circulation in the Skagerrak and more widely in the southern North Sea with a strong influence of Atlantic Water in the region. This oceanographic development in the Skagerrak is most likely associated with the opening of the Danish Straits (9.3–8.1 cal. ka BP; Table 1; Björck 1995; Berglund *et al.* 2005; Gyllencreutz *et al.* 2006) and inflow of water from the Atlantic through the opening of the English Channel across the southern North Sea into the Baltic Sea region (7.7–9.7 cal. ka BP; Table 1; Nordberg 1991; Jiang *et al.* 1997; Gyllencreutz 2005;

Gyllencreutz *et al.* 2006). This opening up of gateways for ocean circulation would encourage stronger exchange between the Kattegat, Skagerrak, and North Sea. This is also supported by the levels of $\%C_{37:4}$ in 372650 remaining relatively high until ~8.5 cal. ka BP, where values abruptly decrease to <2% (Fig. 3). This indicates a reduced freshwater flux into the region and the general development into the more open marine environment of the Skagerrak today. This decrease in $\%C_{37:4}$ may also partly reflect the shift in Baltic drainage/outflow from the more proximal south-central Sweden pathway to the more distal Danish Straits, hence diluting the freshwater signal over an increased distance. The reduced freshwater flux is also supported by the $^{187}Os/^{188}Os$ ratio, which, by this time, has decreased to stabilize at values closer to an open marine signal ~1 through much of the Middle Holocene in cores M86-5 and M86-7 (Fig. 4).

Further implications: conservative vs. non-conservative behaviour of Os

In contrast to Re, whose abundances remain relatively stable from core bottom to top (1.84–1.75 and 0.76–1.74 ppb for M86-5 and M86-7, respectively), the total osmium abundance increases from core bottom to top (74–140 and 70–140 ppt in M86-5 and M86-7, respectively and 65–85 ppt in M86-6 between 6.6 and 5.4 m; Fig. 4). The total Os values are relatively stable near the base of the core until ~7 m in M86-5 and ~6.3 m in M86-7, before beginning to increase. Rising total Os values coincide with a decrease in $^{187}Os/^{188}Os$ values and $\%C_{37:4}$ representing a gradual increase in marine influence and a decrease in freshwater influence (Figs 3, 4). This is therefore inferred to represent a gradually increasing water column salinity from the core bottom to the core top. Diatom studies of salinity in the Skagerrak (and Kattegat) have found significant amounts of freshwater discharge during the Younger Dryas from the Baltic Ice Lake, and then increased salinity through the Holocene (Jiang *et al.* 1998a, b). This interval corresponds in time to the deepest sections of the M86 cores, where the Os abundances are at their lowest, and hence support a lower salinity during this time.

Although the conservative or non-conservative (increases or no trend with salinity, respectively) behaviour of osmium is debated, based on studies from different global locations (e.g. Levasseur *et al.* 2000; Turekian *et al.* 2007; Sproson *et al.* 2018; Ownsworth *et al.* 2019), the relationship observed in this study would appear to support the conservative behaviour of osmium.

Conclusions

Using several cores from across the Skagerrak, chronostratigraphically linked via benthic foraminifera markers and typical features in XRF, carbonate and grain size, this study presents evidence for several events occurring through the Lateglacial to Middle Holocene including a large freshwater input, the Glomma River drainage event and the opening of the Danish Strait and English Channel. Based on the proxies presented here in two Skagerrak cores (percentage sand content, Ca/K, TIC, $\%C_{37:4}$, foraminifera data and $^{187}Os/^{188}Os$), an increased input of cold, radiogenic fresh water is recorded with an increase in grain size and is broadly constrained with radiocarbon dating to between <13.3 and 11.3 cal. ka BP. This could be due to increased iceberg discharge and meltwater input from the retreating SIS, which could also have remobilized previously deposited sand-rich layers. A potential contribution may also have come from the drainage of the BIL that occurred during this time interval (11.6 cal. ka BP). At 9.9 cal. ka BP a sudden appearance of *Valvulineria* as well as higher $\%C_{37:4}$ values imply an organic freshwater fluvial input, corresponding in timing to the Glomma drainage event from southern Norway. The appearance of *H. balthica* and fall in $\%C_{37:4}$ at 8.5 cal. ka BP shows the transition of the Skagerrak into its modern-day configuration and circulation patterns, coincident with the opening of the Danish Straits and the English Channel.

This study supports earlier research (e.g. Heier-Nielsen *et al.* 1995; Knudsen *et al.* 1996) showing that AMS ^{14}C dating of benthic foraminifera may provide inaccurate results because of sediment re-working and re-deposition, not only during the formation of sand layers. However, when considering the site-specific sedimentation rate and the appearance of certain benthic foraminifera (e.g. *H. balthica* and potentially *Valvulineria*), dating of monospecific samples appears useful in core intervals where mollusc shells are not available. We present a stratigraphic approach using benthic foraminifera to create a chronostratigraphic framework across the Skagerrak. We show that several cores, spread across the Skagerrak, all show remarkably similar patterns in foraminifera species, suggesting that they are universal markers across a large proportion of the Skagerrak and therefore could be used to correlate Early Holocene core intervals in the entire Skagerrak. This may allow the development of a master chronology with a high temporal resolution in future studies.

Data availability statement. – The data that support the findings of this study are available in a data repository that will be linked to the article.

References

Andrén, E., Andrén, T. & Kunzendorf, H. 2000: Holocene history of the Baltic Sea as a background for assessing records of human impact in the sediments of the Gotland Basin. *Holocene 10*, 687–702.

Andrén, T., Björck, S., Andrén, E., Conley, D., Zillén, L. & Anjar, J. 2011: The development of the Baltic Sea Basin during the last 130 ka. *In* Harff, J., Björck, S. & Hoth, P. (eds.): *The Baltic Sea Basin*, 75–98. Springer, Berlin Heidelberg.

Andrén, T. and 33 others 2015: *Expedition 347 summary*. IODP.

Andrén, T., Lindeberg, G. & Andrén, E. 2002: Evidence of the final drainage of the Baltic Ice Lake and the brackish phase of the Yoldia Sea in glacial varves from the Baltic Sea. *Boreas 31*, 226–238.

Bendle, J., Rosell-Melé, A. & Ziveri, P. 2005: Variability of unusual distributions of alkenones in the surface waters of the Nordic seas. *Paleoceanography 20*, 1–15.

Bennike, O. & Jensen, J. B. 2013: A Baltic Ice Lake lowstand of latest Allerød age in the Arkona basin, southern Baltic sea. *Geological Survey of Denmark and Greenland Bulletin 28*, 17–20.

Berglund, B. E., Sandgren, P., Barnekow, L., Hannon, G., Jiang, H., Skog, G. & Yu, S. Y. 2005: Early Holocene history of the Baltic Sea, as reflected in coastal sediments in Blekinge, southeastern Sweden. *Quaternary International 130*, 111–139.

Björck, S. 1995: A review of the history of the Baltic Sea, 13.0-8.0 ka BP. *Quaternary International 27*, 19–40.

Björck, S., Andrén, T. & Jensen, J. B. 2008: An attempt to resolve the partly conflicting data and ideas on the Ancylus-Littorina transition. *Polish Geological Institute Special Papers 23*, 21–26.

Björck, S., Koç, N. & Skog, G. 2003: Consistently large marine reservoir ages in the Norwegian Sea during the Last Deglaciation. *Quaternary Science Reviews 22*, 429–435.

Bodén, P., Fairbanks, R. G., Wright, J. D. & Burckle, L. H. 1997: High-resolution stable isotope records from southwest Sweden: The drainage of the Baltic Ice Lake and Younger Dryas Ice Margin Oscillations. *Paleoceanography 12*, 39–49.

Bøe, R., Rise, L., Thorsnes, H., de Haas, H., Sæther, H. & Kunzendorf, H. 1996: Sea-bed sediments and sediment accumulation rates in the Norwegian part of the Skagerrak. *Geological Survey of Norway Bulletin 430*, 75–84.

Burton, K. W., Bourdon, B., Birck, J. L., Allègre, C. J. & Hein, J. R. 1999: Osmium isotope variations in the oceans recorded by Fe-Mn crusts. *Earth and Planetary Science Letters 171*, 185–197.

Burton, K. W., Gannoun, A. & Parkinson, I. J. 2010: Climate driven glacial-interglacial variations in the osmium isotope composition of seawater recorded by planktic foraminifera. *Earth and Planetary Science Letters 295*, 58–68.

CALIB rev. 8, Stuiver, M. & Reimer, P. J. 1993: Radiocarbon. 35 215–230, http://calib.org/calib/.

Chen, C., Sedwick, P. N. & Sharma, M. 2009: Anthropogenic osmium in rain and snow reveals global-scale atmospheric contamination. *Proceedings of the National Academy of Sciences of the United States of America 106*, 7724–7728.

Cohen, A. S. 2004: The rhenium-osmium isotope system: applications to geochronological and palaeoenvironmental problems. *Journal of the Geological Society 161*, 729–734.

Cohen, A. S., Coe, A. L., Bartlett, J. M. & Hawkesworth, C. J. 1999: Precise Re-Os ages of organic-rich mudrocks and the Os isotope composition of Jurassic seawater. *Earth and Planetary Science Letters 167*, 159–173.

Croudace, I. W., Rindby, A. & Rothwell, R. G. 2006: ITRAX: description and evaluation of a new multi-function X-ray core scanner. *Geological Society, Special Publications 267*, 51–63.

Demina, L. L., Novichkova, K. A., Lisitzin, A. P. & Kozina, N. V. 2019: Geochemical signatures of paleoclimate changes in the sediment cores from the gloria and snorri drifts (Northwest Atlantic) over the Holocene-mid Pleistocene. *Geosciences 9*, 432, https://doi.org/10.3390/geosciences9100432.

Dickens, A. W. 2013: *Late Quaternary Palaeoceanographic Evolution in the Skagerrak, Northeastern North Sea*. Durham University, Durham. Available at: http://etheses.dur.ac.uk/6934/.

Du Vivier, A. D. C., Selby, D., Sageman, B. B., Jarvis, I., Gröcke, D. R. & Voigt, S. 2014: Marine 187Os/188Os isotope stratigraphy reveals the interaction of volcanism and ocean circulation during Oceanic Anoxic Event 2. *Earth and Planetary Science Letters 389*, 23–33.

Ducrotoy, J. & Elliott, M. 2008: The science and management of the North Sea and the Baltic Sea: natural history, present threats and future challenges. *Marine Pollution Bulletin 57*, 8–21.

EMODnet 2023: *EMODnet*. European Commission. Available at: https://emodnet.ec.europa.eu/geoviewer/.

Erbs-Hansen, D. R., Knudsen, K. L., Gary, A. C., Jansen, E., Gyllencreutz, R., Scao, V. & Lambeck, K. 2011a: Fe/Ti and Ca/K ratios of sediment core MD99-2286. *PANGAEA*, https://doi.org/10.1594/PANGAEA.756231.

Erbs-Hansen, D. R., Knudsen, K. L., Gary, A. C., Jansen, E., Gyllencreutz, R., Scao, V. & Lambeck, K. 2011b: Late Younger Dryas and early Holocene palaeoenvironments in the Skagerrak, eastern North Atlantic: a multiproxy study. *Boreas 40*, 660–680.

Erlenkeuser, H. 1985: Stable isotopes in benthic foraminifers of Skagerrak core GIK-15530-4: Heigh resolution record of the Younger Dryas and Holocene. *Norsk Geologisk Tidsskrift 65*, 49–57.

Etourneau, J., Schneider, R., Blanz, T. & Martinez, P. 2010: Intensification of the Walker and Hadley atmospheric circulations during the Pliocene-Pleistocene climate transition. *Earth and Planetary Science Letters 297*, 103–110.

Frezza, V., Bergamin, L. & Di Bella, L. 2005: Opportunistic benthic foraminifera as indicators of eutrophicated environments. Actualistic study and comparison with the Santernian middle Tiber Valley (Central Italy). *Bollettino della Societa Paleontologica Italiana 44*, 193–201.

Gannoun, A. & Burton, K. W. 2014: High precision osmium elemental and isotope measurements of North Atlantic seawater. *Journal of Analytical Atomic Spectrometry 29*, 2330–2342.

Guilderson, T. P., Reimer, P. J. & Brown, T. A. 2005: The boon and bane of radiocarbon dating. *Science 307*, 362–364.

Gyllencreutz, R. 2005: Late Glacial and Holocene paleoceanography in the Skagerrak from high-resolution grain size records. *Palaeogeography, Palaeoclimatology, Palaeoecology 222*, 344–369.

Gyllencreutz, R., Backman, J., Jakobsson, M., Kissel, C. & Arnold, E. 2006: Postglacial palaeoceanography in the Skagerrak. *The Holocene 16*, 975–985.

Hald, M. & Korsun, S. 1997: Distribution of modern benthic foraminifera from fjords of Svalbard, European Arctic. *Journal of Foraminiferal Research 27*, 101–122.

Hebbeln, D., Knudsen, K. L., Gyllencreutz, R., Kristensen, P., Klitgaard-Kristensen, D., Backman, J., Scheurle, C., Jiang, H., Gil, I., Smelror, M., Jones, P. D. & Sejrup, H.-P. 2006: Late Holocene coastal hydrography and climate changes in the eastern North Sea. *The Holocene 16*, 987–1001.

Heier-Nielsen, S., Heinemeier, J., Nielsen, H. L. & Rud, N. 1995: Recent reservoir ages for Danish fjords and marine waters. *Radiocarbon 37*, 875–882.

Høgaas, F. & Longva, O. 2018: The late-glacial ice-dammed lake Nedre Glomsjø in Mid-Norway: an open lake system succeeding an actively retreating ice sheet. *Norwegian Journal of Geology 98*, 661–675.

Høgaas, F., Hansen, L., Berthling, I., Klug, M., Longva, O., Nannestad, H. D., Olsen, L. & Romundset, A. 2023: Timing and maximum flood level of the Early Holocene glacial lake Nedre Glomsjø outburst flood, Norway. *Boreas 52*, 295–313.

Jakobsson, M., Björck, S., Alm, G., Andrén, T., Lindeberg, G. & Svensson, N. O. 2007: Reconstructing the Younger Dryas ice dammed lake in the Baltic Basin: bathymetry, area and volume. *Global and Planetary Change 57*, 355–370.

Jansen, J. H. F., van Weering, T. C. E. & Eisma, D. 1979: Late Quaternary sedimentation in the North Sea. *In* Oele, E., Schüttenhelm, R. T. E. & Wiggers, A. J. (eds.): *The Quaternary History of the North Sea*, 175–187. Upsala University, Upsala.

Jennings, A. E. & Helgadottir, G. 1994: Foraminiferal assemblages from the fjords and shelf of eastern Greenland. *The Journal of Foraminiferal Research 24*, 123–144.

Jennings, A., Andrews, J., Reilly, B., Walczak, M., Jakobsson, M., Mix, A., Stoner, J., Nicholls, K. W. & Cheseby, M. 2020: Modern foraminiferal assemblages in northern Nares Strait, Petermann Fjord, and beneath Petermann ice tongue, NW Greenland. *Arctic, Antarctic, and Alpine Research 52*, 491–511.

Jiang, H., Björck, S. & Knudsen, K. L. 1997: A palaeoclimatic and palaeoceanographic record of the last 11 000 ^{14}C years from the Skagerrak-Kattegat, northeastern Atlantic margin. *Holocene 7*, 301–310.

Jiang, H., Björck, S. & Svensson, N.-O. 1998a: Reconstruction of Holocene sea-surface salinity in the Skagerrak–Kattegat: a climatic and environmental record of Scandinavia. *Journal of Quaternary Science 13*, 107–114.

Jiang, H., Svensson, N.-O. & Björck, S. 1998b: Meltwater discharge to the Skagerrak–Kattegat from the Baltic Ice Lake during the Younger Dryas interval. *Quaternary Research 49*, 264–270.

Johnson, M. D., Öhrling, C., Bergström, A., Dreyer Isaksson, O. & Pizarro Rajala, E. 2022: Geomorphology and sedimentology of features formed at the outlet during the final drainage of the Baltic Ice Lake. *Boreas 51*, 20–40.

Johnson, M. D., Ståhl, Y., Larsson, O. & Seger, S. 2010: New exposures of Baltic Ice Lake drainage sediments, Götene, Sweden. *GFF 132*, 1–12.

Klitgaard-Kristensen, D., Sejrup, H. F. & Haflidason, H. 2002: Distribution of recent calcareous benthic foraminifera in the northern North Sea and relation to the environment. *Polar Research 21*, 275–282.

Knudsen, K. L. 1984: Foraminiferal stratigraphy in a marine Eemian-Weichselian sequence at Apholm, North Jutland. *Bulletin of the Geological Society of Denmark 32*, 169–180.

Knudsen, K. L., Conradsen, K., Heier-Nielsen, S. & Seidenkrantz, M. S. 1996: Palaeoenvironments in the Skagerrak-Kattegat basin in the eastern North Sea during the last deglaciation. *Boreas 25*, 65–78.

Korsun, S. & Hald, M. 1998: Modern benthic foraminifera off Novaya Zemlya tidewater glaciers, Russian Arctic. *Arctic and Alpine Research 30*, 61–77.

Krossa, V. R., Moros, M., Blanz, T., Jansen, E. & Schneider, R. 2015: Late Holocene Baltic Sea outflow changes reconstructed using C37:4 content from marine cores. *Boreas 44*, 81–93.

Kuroda, J., Jiménez-Espejo, F. J., Nozaki, T., Gennari, R., Lugli, S., Manzi, V., Roveri, M., Flecker, R., Sierro, F. J., Yoshimura, T., Suzuki, K. & Ohkouchi, N. 2016: Miocene to Pleistocene osmium isotopic records of the Mediterranean sediments. *Paleoceanography 31*, 148–166.

Larsson, O., Stevens, R. L. & Klingberg, F. 2007: The transition from glacimarine to marine conditions during the last deglaciation in eastern Skagerrak. *Marine Geology 241*, 45–61.

Levasseur, S. 1998: Direct measurement of femtomoles of osmium and the 187Os/186Os ratio in seawater. *Science 282*, 272–274.

Levasseur, S., Birck, J. L. & Allègre, C. J. 1999: The osmium riverine flux and the oceanic mass balance of osmium. *Earth and Planetary Science Letters 174*, 7–23.

Levasseur, S., Rachold, V., Birck, J. L. & Allègre, C. J. 2000: Osmium behavior in estuaries: the Lena River example. *Earth and Planetary Science Letters 177*, 227–235.

Lloyd, J. M. 2006: Modern distribution of benthic foraminifera from Disko Bugt, West Greenland. *The Journal of Foraminiferal Research 36*, 315–331.

Longva, O. 1994: *Flood Deposits and Erosional Features from the Catastrophic Drainage of Preboreal Glacial Lake Nedre Glåmsjø, SE Norway.* Department of Geology, University of Bergen, Bergen.

Longva, O. & Bakkejord, K. J. 1990: Iceberg deformation and erosion in soft sediments, southeast Norway. *Marine Geology 92*, 87–104.

Longva, O. & Thoresen, M. K. 1991: Iceberg scours, iceberg gravity craters and current erosion marks from a gigantic Preboreal flood in southeastern Norway. *Boreas 20*, 47–62.

Luguet, A., Nowell, G. M. & Pearson, D. G. 2008: ^{184}Os/^{188}Os and ^{186}Os/^{188}Os measurements by Negative Thermal Ionisation Mass Spectrometry (N-TIMS): effects of interfering element and mass fractionation corrections on data accuracy and precision. *Chemical Geology 248*, 342–362.

Mangerud, J. 1972: Radiocarbon dating of marine shells, including a discussion of apparent age of recent shells from Norway. *Boreas 1*, 143–172.

Mangerud, J. & Gulliksen, S. 1975: Apparent radiocarbon ages of recent marine shells from Norway, Spitsbergen, and Arctic Canada. *Quaternary Research 5*, 263–273.

Mojtahid, M., Griveaud, C., Fontanier, C., Anschutz, P. & Jorissen, F. J. 2010: Live benthic foraminiferal faunas along a bathymetrical transect (140–4800m) in the Bay of Biscay (NE Atlantic). *Revue de Micropaleontologie 53*, 139–162.

Morigi, C., Jorissen, F. J., Fraticelli, S., Horton, B. P., Principi, M., Sabbatini, A., Capotondi, L., Curzi, P. V. & Negri, A. 2005: Benthic foraminiferal evidence for the formation of the Holocene mud-belt and bathymetrical evolution in the central Adriatic Sea. *Marine Micropaleontology 57*, 25–49.

Moros, M., Lloyd, J. M., Perner, K., Krawczyk, D., Blanz, T., de Vernal, A., Ouellet-Bernier, M. M., Kuijpers, A., Jennings, A. E., Witkowski, A., Schneider, R. & Jansen, E. 2016: Surface and sub-surface multi-proxy reconstruction of middle to late Holocene palaeoceanographic changes in Disko Bugt, West Greenland. *Quaternary Science Reviews 132*, 146–160.

Muschitiello, F., Lea, J. M., Greenwood, S. L., Nick, F. M., Brunnberg, L., MacLeod, A. & Wohlfarth, B. 2016: Timing of the first drainage of the Baltic Ice Lake synchronous with the onset of Greenland Stadial 1. *Boreas 45*, 322–334.

Nordberg, K. 1991: Oceanography in the Kattegat and Skagerrak over the past 8000 years. *Paleoceanography 6*, 461–484.

Nowell, G. M., Luguet, A., Pearson, D. G. & Horstwood, M. S. A. 2008: Precise and accurate ^{186}Os/^{188}Os and ^{187}Os/^{188}Os measurements by multi-collector plasma ionisation mass spectrometry (MC-ICP-MS) part I: solution analyses. *Chemical Geology 248*, 363–393.

Olsen, J., Rasmussen, P. & Heinemeier, J. 2009: Holocene temporal and spatial variation in the radiocarbon reservoir age of three Danish fjords. *Boreas 38*, 458–470.

Ownsworth, E., Selby, D., Lloyd, J., Knutz, P., Szidat, S., Andrews, J. & Ó Cofaigh, C. 2023: Tracking sediment delivery to central Baffin Bay during the past 40 kyrs: insights from a multiproxy approach and new age model. *Quaternary Science Reviews 308*, 108082, https://doi.org/10.1016/j.quascirev.2023.108082.

Ownsworth, E., Selby, D., Ottley, C. J., Unsworth, E., Raab, A., Feldmann, J., Sproson, A. D., Kuroda, J., Faidutti, C. & Bücker, P. 2019: Tracing the natural and anthropogenic influence on the trace elemental chemistry of estuarine macroalgae and the implications for human consumption. *Science of the Total Environment 685*, 259–272.

Oxburgh, R. 1998: Variations in the osmium isotope composition of seawater over the past 200 000 years. *Earth and Planetary Science Letters 159*, 183–191.

Oxburgh, R. 2001: Residence time of osmium in the oceans. *Geochemistry, Geophysics, Geosystems 2*, 1–17, https://doi.org/10.1029/2000GC000104.

Paquay, F. S. & Ravizza, G. 2012: Heterogeneous seawater ^{187}Os/^{188}Os during the Late Pleistocene glaciations. *Earth and Planetary Science Letters 349–350*, 126–138.

Petersen, K. S., Rasmussen, K. L., Rasmussen, P. & von Platen-Hallermund, F. 2005: Main environmental changes since the Weichselian glaciation in the Danish waters between the North Sea and the Baltic Sea as reflected in the molluscan fauna. *Quaternary International 133–134*, 33–46.

Peucker-Ehrenbrink, B. & Ravizza, G. 1996: Continental runoff of osmium into the Baltic Sea. *Geology 24*, 327–330.

Peucker-Ehrenbrink, B. & Ravizza, G. 2000: The marine osmium isotope record. *Terra Nova 12*, 205–219.

Peucker-Ehrenbrink, B. & Ravizza, G. 2012: Osmium isotope stratigraphy. *In* Gradstein, F. M., Ogg, J. G., Schmitz, M. D. & Ogg, G. M. (eds.): *The Geologic Time Scale*, 145–166. Elsevier, Amsterdam.

Qvale, G. & van Weering, T. C. E. 1985: Relationship of surface sediments and benthic foraminiferal distribution patterns in the Norwegian Channel (northern North Sea). *Marine Micropaleontology 9*, 469–488.

Ravizza, G. & Turekian, K. K. 1989: Application of the 187Re–187Os system to black shale geochronometry. *Geochimica et Cosmochimica Acta 53*, 3257–3262.

Rodhe, J. & Holt, N. 1996: Observations of the transport of suspended matter into the Skagerrak along the western and northern Coast of Jutland. *Journal of Sea Research 35*, 91–98.

Rooney, A. D., Selby, D., Lloyd, J. M., Roberts, D. H., Lückge, A., Sageman, B. B. & Prouty, N. G. 2016: Tracking millennial-scale Holocene glacial advance and retreat using osmium isotopes: insights from the Greenland ice sheet. *Quaternary Science Reviews 138*, 49–61.

Rosell-Melé, A. 1998: Interhemispheric appraisal of the value of alkenone indices as temperature and salinity proxies in high-latitude locations. *Paleoceanography 13*, 694–703.

Rosell-Melé, A., Jansen, E. & Weinelt, M. 2002: Appraisal of a molecular approach to infer variations in surface ocean freshwater inputs into the North Atlantic during the last glacial. *Global and Planetary Change 34*, 143–152.

Rosentau, A., Bennike, O., Uscinowicz, S. & Miotk-Szpiganowicz, G. 2017: The Baltic Sea Basin. *In* Flemming, N. C., Harff, J., Moura, D., Burgess, A. & Bailey, G. N. (eds.): *Submerged Landscapes of the European Continental Shelf: Quaternary Paleoenvironments*, 103–133. Willey & Sons Ltd, Chichester.

Rothwell, R. G. & Croudace, I. W. 2015: Twenty years of XRF core scanning marine sediments: what do geochemical proxies tell us? *In* Rothwell, R. G. & Croudace, I. W. (eds.): *Micro-XRF Studies of Sediment Cores 17*, 25–102. Springer, Dordrecht.

Selby, D. & Creaser, R. A. 2003: Re–Os geochronology of organic rich sediments: an evaluation of organic matter analysis methods. *Chemical Geology 200*, 225–240.

Sharma, M., Papanastassiou, D. A. & Wasserburg, G. J. 1997: The concentration and isotopic composition of osmium in the oceans. *Geochimica et Cosmochimica Acta 61*, 3287–3299.

Sicre, M.-A., Bard, E., Ezat, U. & Rostek, F. 2002: Alkenone distributions in the North Atlantic and Nordic sea surface waters. *Geochemistry, Geophysics, Geosystems 3*, 1–13.

Solheim, A. & Grønlie, G. 1983: Quaternary sediments and bedrock geology in the outer Oslofjord and northernmost Skagerrak. *Norsk Geologisk Tidsskrift 63*, 55–71.

Sproson, A. D., Pogge von Strandmann, P. A. E., Selby, D., Jarochowska, E., Frýda, J., Hladil, J., Loydell, D. K., Slavík, L., Calner, M., Maier, G., Munnecke, A. & Lenton, T. M. 2022: Osmium and lithium isotope evidence for weathering feedbacks linked to orbitally paced organic carbon burial and Silurian glaciations. *Earth and Planetary Science Letters 577*, 117260, https://doi.org/10.1016/j.epsl.2021.117260.

Sproson, A. D., Selby, D., Gannoun, A., Burton, K. W., Dellinger, M. & Lloyd, J. M. 2018: Tracing the impact of coastal water geochemistry on the Re-Os systematics of macroalgae: insights from the basaltic terrain of Iceland. *Journal of Geophysical Research: Biogeosciences 123*, 2791–2806.

Stroeven, A. P., Heyman, J., Fabel, D., Björck, S., Caffee, M. W., Fredin, O. & Harbor, J. M. 2015: A new Scandinavian reference 10Be production rate. *Quaternary Geochronology 29*, 104–115.

Strömberg, B. 1992: The final stage of the Baltic Ice Lake. *Sveriges Geologiska Undersökning 81*, 347–353.

Swärd, H., O'Regan, M., Ampel, L., Ananyev, R., Chernykh, D., Floden, T., Greenwood, S. L., Kylander, M. E., Mörth, C. M., Preto, P. & Jakobsson, M. 2015: Regional deglaciation and postglacial lake development as reflected in a 74 m sedimentary record from Lake Vättern, southern Sweden. *GFF 138*, 336–354.

Turekian, K. K., Sharma, M. & Gordon, G. W. 2007: The behavior of natural and anthropogenic osmium in the Hudson River-Long Island Sound estuarine system. *Geochimica et Cosmochimica Acta 71*, 4135–4140.

van Weering, T. C. E. 1982: Recent sediments and sediment transport in the northern North Sea; pistoncores from the Skagerrak. *Proceedings of the Koninklijke Nederlandse Akademie van Wetenschappen 85*, 155–201.

van Weering, T. C. E., Berger, G. W. & Okkels, E. 1993: Sediment transport, resuspension and accumulation rates in the northeastern Skagerrak. *Marine Geology 111*, 269–285.

Supporting Information

Additional Supporting Information to this article is available at http://www.boreas.dk.

Data S1. Methods of core correlation and dating of tie points.

Data S2. Core correlation tie points in cores M86-6, M86-7 and MD99-2286.

Data S3. Core correlation tie points in cores M86-5, 372650 and 242940.

Data S4. Core correlation tie points in core Skagen-3.

Table S1. Sample type and depth used for radiocarbon dating.